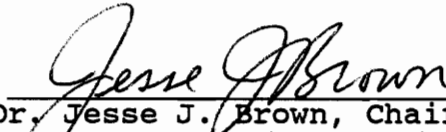# ALKALI ATTACK ON CERAMIC FILTERS

by

Raymond J. Vass

Thesis submitted to the Faculty of the

Virginia Polytechnic Institute and State University

in partial fulfillment of the requirements for the degree of

MASTER OF SCIENCE

in

Materials Engineering

APPROVED:

Dr. Jesse J. Brown, Chairman,
Professor, Materials Engineering

Dr. Robert Swanson,
Associate Professor,
Materials Engineering

Dr. Diana Farkas,
Associate Professor,
Materials Engineering

December 1990

Blacksburg, Virginia

ALKALI ATTACK ON CERAMIC FILTERS

by

Raymond J. Vass

Committee Chairman: Dr. Jesse Brown
Materials Engineering

(ABSTRACT)

Experiments were performed to determine a suitable binder material for silicon carbide-based ceramic filter. These experiments included exposure of 42% and 60% alumina, aluminosilicates to potassium and sodium containing environments for the purpose of determining the phases that would form and to determine concentration profiles. In addition, thermodynamic calculations were performed to predict the phases that would form when the alkali reacted with the aluminosilicate.

The results of the thermodynamic calculations indicated that the alkali compounds will react at temperatures as low as 800°C. The exposure experiments verified this result. The phases that formed during the sodium vapor exposures and confirmed the thermodynamic calculations and were as follows:
1.   sodium metasilicate and a solid solution of sodium aluminum silicates and carnegieite and for potassium vapor exposure.

2. potassium disilicate, kaliophilite-nepheline,
potassium aluminate, and $5K_2O-5Al_2O_3-8SiO_2$.
Experiments also revealed that penetration depth by alkali
compounds was restricted to a region near the surface of
the material when the combination of temperature and
sodium concentration alowed a melt to form.

The results also indicated that the 42% alumina,
aluminosilicate had superior resistance to alkali attack
than the 60% alumina, aluminosilicate at temperatures
below 1225°C.

ACKNOWLEDGMENTS

I would like to thank Dr. Jesse J. Brown for his support and direction in this research endeavor.

Special thanks to Nancy Brown for her dedicated work on this project.

I am also indebted to Dr. Swanson and Dr. Farkas for serving on my committee.

Special gratitude extended to Ruth and Bob Holman for their team effort on my behalf.

Heartfelt thanks to Dr. Tawei Sun for wise words, good conversation, and friendship.

To my parents, Stanley and Wilma Vass, I extend deep gratitude for their love and interest in my research progress.

I wish to thank my wife, Dianna, for going through our master's programs together and making me strive for intellectual excellence.

TABLE OF CONTENTS

LIST OF TABLES

I. INTRODUCTION

A. Background Information

The selection of ceramic filter materials that will provide durability for extended use in hot gas cleanup devices is critical to the success of advanced coal combustion processes. Several types of filters have been developed which demonstrate efficient particulate removal for short periods of time, but then experience failure. From this standpoint, the environment established by coal combustion and its interactions with materials are of interest. One of several proposed materials are aluminosilicates, which would be use as a binder material in a ceramic filter. The exposure of such materials to a high temperature combustion environment will strongly affect the service life of the ceramic filters.

The environment that the filters will encounter contains gases such as hydrogen, methane, carbon oxides, steam, and sulfur-containing constituents. In addition to the gases, the ceramic filters will be exposed to a variety of solid particles (coal dust, slag, etc.) containing several metallic compounds. These compounds contain metals such as: sodium, potassium, iron, calcium, and zinc. Strength loss has been known to occur in ceramic materials exposed to similar environments.

Chemical attack of ceramics is a primary limiting factor in their long-term use at high temperatures. In general, ceramic or refractory materials are known to be

1

chemically inert under a variety of conditions at high temperatures. However, at high temperatures the ceramics may become susceptible to chemical degradation. There have been several cases where an inappropriate choice of materials for the conditions involved resulted in premature and/or catastrophic failure such as at the Grand Forks slagging gasifier where a refractory lining failed after only 125 h of service.[1]

The corrosion of aluminosilicates by alkali compounds has been extensively studied. It has been found that refractory materials react with a number of alkali compounds such as oxides, hydrides, and carbonates of potassium and/or sodium.[2] A typical reaction proposed by Kennedy[1] is shown below:

$$11(Al_6Si_2O_{13}) + 26(NaOH) \longrightarrow 22(NaAlSiO4) + 13H_2O \quad (1)$$
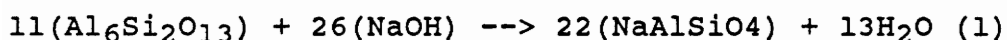
This type of reaction leads to large volume expansion and subsequent spalling or cracking of the material. Similar reactions occur with potassium compounds. Calcium has also been found to cause degradation, but does not appear to be as reactive as sodium or potassium.

Wei et al.[3] studied the effects of coal combustion environments on high-duty fireclay refractories (~37% alumina). The fireclay brick was used in a coal-fired periodic kiln. The reaction products found on the exposed side of the brick consisted of a glassy phase with crystals of a sodium-calcium-alumina-silicate. Other phases included corundum, mullite, and

cristobalite. The glassy slag was found to have a high alkali content. This surface slag is believed to form when alkali reacts with free silica to form low melting eutectics. Mullite is also attacked and dissociates into corundum and more free silica. The presence of the glassy slag will protect the brick from further degradation as long as the slag viscosity is high. Wei et al. concluded that high-duty fireclay refractories performed satisfactorily at temperatures below 1260°C.

Hayden[4] studied the reactions of alkali vapors with various aluminosilicate (19-99% Al_2O_3) refractories. She concluded that resistance to alkali attack is increased by increasing alumina content up to 60%; however, increases of alumina content above 60% do not increase resistance to alkali attack. Hayden also stated that the resistance to alkali attack of aluminosilicates containing 60% or less alumina comes about because the reactions form a glassy phase on the surface which tends to seal the surface of the ceramic, preventing deeper penetration of alkali compounds. Further, aluminosilicates with greater than 60% alumina do not have this surface sealing reaction and thus are susceptible to expansive reactions which can cause spalling and/or catastrophic failure.

Farris and Allen[5] studied alkali reactions with aluminosilicate refractory materials ranging from 42-90% Al_2O_3 using sodium and potassium carbonates.

Reactions were found to occur at temperatures as low as 590°C for potassium. Reactions between the potassium oxide and the refractories were found to form potassium aluminum silicates at low temperatures, and potassium aluminates at temperatures above 1100°C. Similar reactions occurred with sodium oxide resulting in the formation of sodium aluminum silicates at low temperature and sodium aluminates at temperatures above 1100°C. These researchers concluded that refractories containing 42-70% alumina have the greatest resistance to alkali attack. Furthermore, for refractories containing more than 50% alumina, a fully-bonded mullite matrix is desirable with as little cristobalite or glass present as possible to achieve maximum alkali resistance.

A study of alkali attack in blast furnaces by Havranek[6] covered several refractories including aluminosilicates (45-90% alumina). Hot modulus of rupture data were obtained at different temperatures for refractory samples exposed to molten potassium carbonate in a reducing atmosphere for five hours. Their test results showed that mullite-bonded alumina maintained good strength after alkali attack at 1400°C, whereas dense fireclay refractories maintained good strength after alkali attack only at low temperatures.

Rigby et al[7] reported that the presence of vanadium and high porosity adversely affects the alkali resistance of refractories. The results of Federer and Tennery[8]

support this conclusion.   They also found that calcium sulfate along with vanadium pentoxide cause significant corrosion of mullite-based refractories.

Federer[9] identified the following corrosion mechanisms in combustion environments:

1.   Formation of liquid phases from reactions with alkali oxides and vanadium pentoxide in aluminosilicates.

2.   Formation of glassy silicates phases from reactions similar to those mentioned above.

3.   Reaction to SiC with compounds in slag such as Fe_2O_3 and NiO to form iron and nickel silicides.

4.   Lowered viscosity of SiO_2 coatings on SiC by reactions with alkali oxides and SiO_2 layer allows greater transport of oxygen through the layer and thus greater oxidation of the SiC.

5.   Halide attack of SiC causing the possible formation of volatile silicon halides.

6.   Volume expansion caused by the formation of new phases such as Beta-Al_2O_3 can cause mechanical stress leading to failure.   Also, new phases can have large coefficients of thermal expansion which will increase thermal stress in the materials.

B. Computer Calculations

The calculation of thermodynamic equilibrium phases for complex solid-liquid-gas systems has been under development for many years. In 1976, the program SOLGASMIX-PV[10] was developed to calculate the equilibrium compositions of complex systems. The program has been used to model several systems containing fuel gas environment and various ceramic materials.[11-12]

The equilibrium calculations used in the computer program are based on minimizing Gibbs free energy of the system and on the conservation of mass for each element present in the system.

The Gibbs free energy for a given system divided by the gas constant and reaction temperature can be expressed by the following equation:

$$G/RT = \sum_{i=1}^{m} x_i^g [(g°/RT)_i^g + \ln P + \ln(x_i^g/X)] + \sum_{l=1}^{s} x_i^c (g°/RT)_i^c$$

where x_i denotes the mole number of a substance, X is the total number of moles in that phase, and g is the chemical potential of a substance. The superscripts refer to gas phases (g) and condensed phases (c). Combining the mass balance for each element, this equation can then be solved using Lagrange's method to obtain the mole numbers of the equilibrium system.

The computer calculations were performed using a system made up of a gas phase mixtures were made of stoichiometric compounds. The composition of the gas

phase, listed in Table 1, is a simulated fuel gas environment typical of a coal gasifer[13].

The fuel gas environment simulated in these computer calculations also contains alkali compounds, potassium or sodium.

In the coal gasification environment there are several possible reactions which will produce alkali vapors. Examples of these reactions are:

$$Na_2CO_3(s) + 2C(s) = 2Na(g) + 3CO(g)$$

$$Na_2CO_3(s) + H_2O(g) = 2NaOH + 2CO(g)$$

or

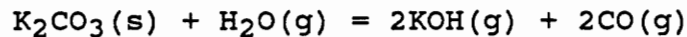$$K_2CO_3(s) + 2C(s) = 2K(g) + 3CO(g)$$

$$K_2CO_3(s) + H_2O(g) = 2KOH(g) + 2CO(g)$$
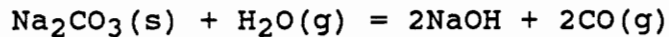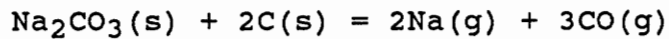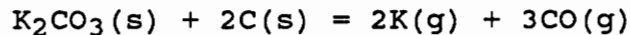
These reactions are affected by both temperature and pressure of the gasifer. Computer calculations have been performed in other studies to determine the stable sodium and potassium compounds, and from these results the phase maps shown in Figures 1 and 2 were prepared.[11] These results indicate that sodium and potassium compounds will be present in the gas phase at temperatures as low as 925°C.

The compounds considered in the computer calculations for sodium and potassium are shown in Tables 2 and 3, respectively. The compounds used to determine stable sodium and potassium vapor phases are included.

Table 1. Composition of Simulated Fuel Gas Atmosphere
(in mole %)

H_2	CH_4	CO	CO_2	H_2O	N_2
12	18	17	12	20	20
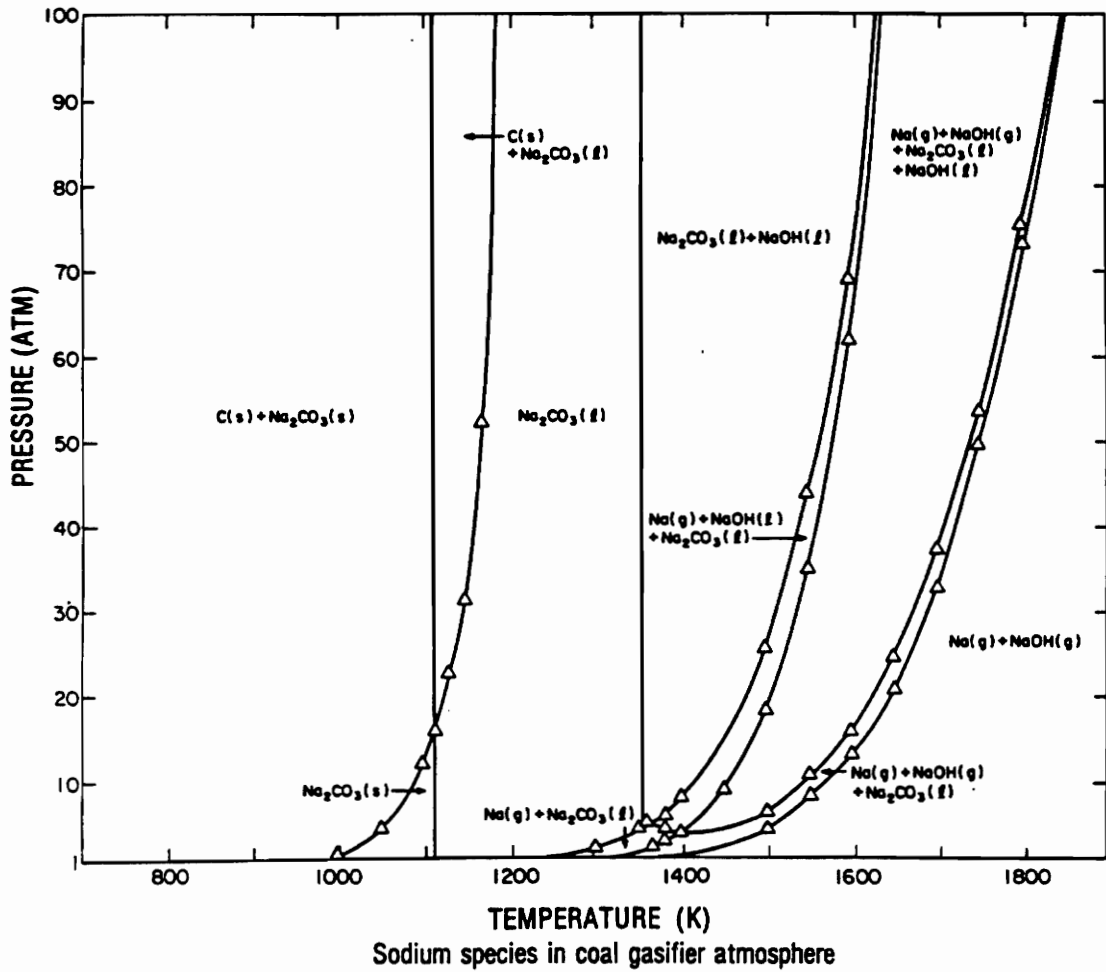
Figure 1. Stable sodium species in coal gasifier atmospheres.[11]

Potassium species in coal gasifier atmosphere
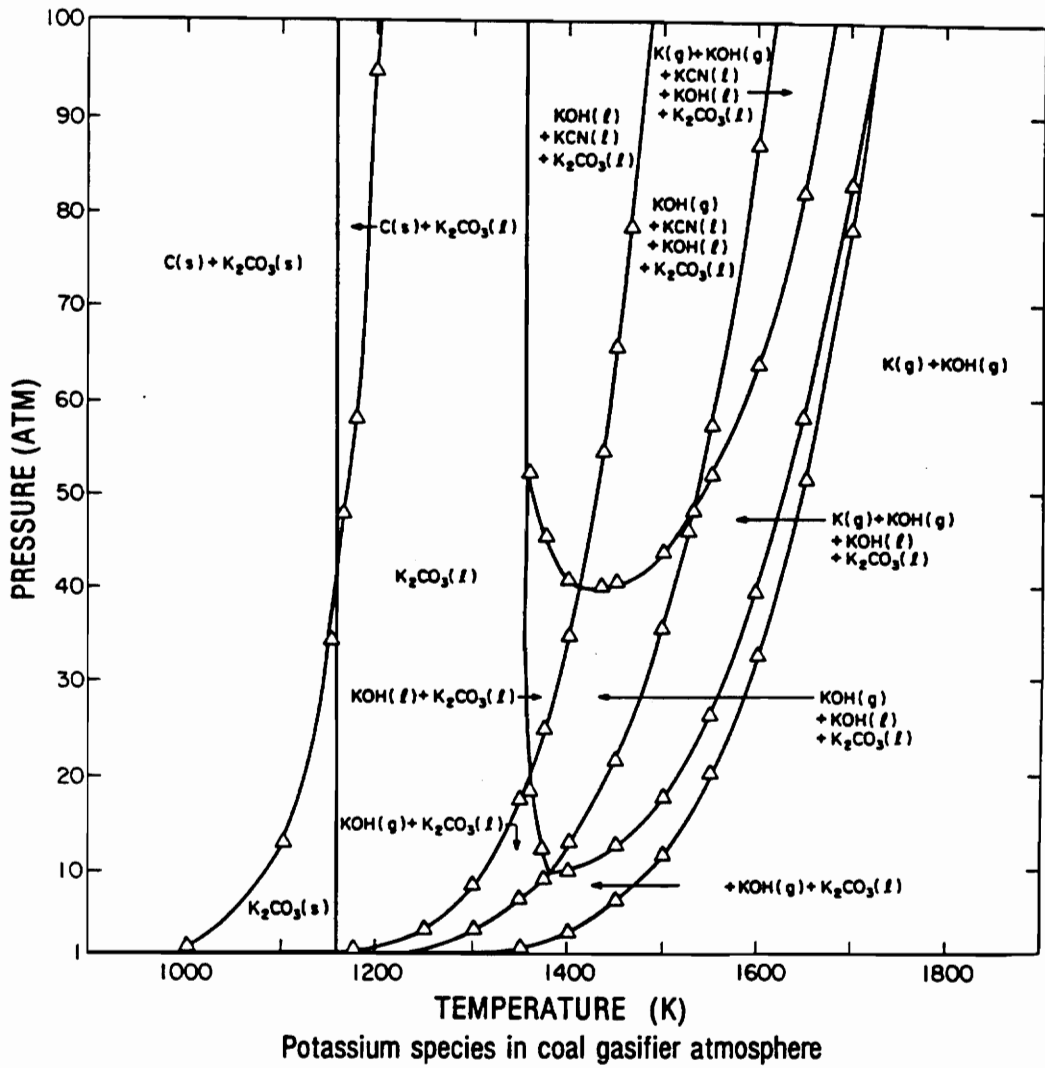
Figure 2.   Stable potassium species in coal gasifier atmospheres.[11]

Table 2. Sodium Compounds Considered in
Thermodynamic Calculations[*]

Gas Phase	Liquid Phase	Solid Phases
Na, Na_2O,	Na, Na_2O, NaOH	Na_2O, NaOH, C
NaOH, NaCN	NaCN	NaCN, Na, NA_{11},
H_2, N_2 CO, NH_3,		NS, NS_2, N_2S, Al
CO_2, O_2, H_2O		NA_8, NAS_6, NAS_2,
		Si, $SiO2$, Al_2O_3,
		A_3S_2

[*]Conventional Cement Chemistry notation used: N=Na_2O,
 S=SiO_2, A=Al_2O_3, K=K_2O

Table 3. Potassium Compounds Considered in
Thermodynamic Calculations[*]

Gas Phase	Liquid Phase	Solid Phases
K, K_2O,	K, K_2O, KOH	K_2O, KOH, C
KOH, KCN	KCN	KCN, K, KA_{11},
H_2, N_2 CO, NH_3,		KS, KS_2, K_4S, Al
CO_2, O_2, H_2O		KAS_6, KAS_2, KAS,
		KAS_4, KA, Si,
		$SiO2$, Al_2O_3, A_3S_2

[*]Conventional Cement Chemistry notation used: $N=Na_2O$,
$S=SiO_2$, $A=Al_2O_3$, $K=K_2O$

II.   EXPERIMENTAL PROCEDURE

The computer calculations using SOLGASMIX-PV are performed using the procedure outlined by Sun[11] and involves the following steps:

1) define the thermodynamic system.

2) define the reference state.

3) input the thermodynamic data for each species in the system, in this case Gibbs free energy of formation from elements.

4) input the chemical formula for each species.

5) specify the total amount (in g-atoms) of each element in the system.

The thermodynamic system defined above consists of gas, liquid, and solid phases that may be present for each of species that make up the system. The thermodynamic data was collected from a variety of sources[14-32] and uses a standard reference state, 273K and 1 atm.

The calculations for sodium and potassium were carried out for the temperatures 725, 925C, and 1225C. The calculation were performed using three molar ratios of alkali to Al_2O_3. These ratios were 1:2, 1:1, and 2:1.

Alkali Exposure Tests

Experiments were performed to study the reactions of sodium and potassium with calcined kaolinite (~ 42% Al_2O_3) and a 60% Al_2O_3 aluminosilicate, which

13

after calcining is primarily mullite. The kaolinite samples were prepared by pressing 20g of powdered kaolin and 1g of cellulose ether as a binder into 1 x 1 x 10 cm bars using a hydraulic press and 10000 psi of pressure. The bars were then calcined for 48 h at 1225°C and subsequently cut in half to form 1 x 1 x 5 cm sample bars.

Mullite samples were prepared using 18.4 g $Al(OH)_3$ and 9.3 g silicic acid and 1 g cellulose ether. This mixture was pressed into 1 x 1 x 10 cm bars at 12000 psi and calcined at 1550°C for 48 h. The bars were then ground with 1 g of cellulose ether, pressed into 1 x 1 x 10 cm bars at 12000 psi and fired at 1600°C for 48 h. Then samples were cut into 1 x 1 x 5 cm bars for exposure tests.

The sample bars were each fired at different temperatures and different firing times in the presence of either 3 g of Na_2CO_3 or 4 g of K_2CO_3 placed separately in the tube furnace to provide an alkali source. A schematic of the test apparatus is shown in Figure 3. After exposure to alkali environment, the samples were analyzed using XRD and EDX. In addition, samples were examined optically using a polarizing microscope to confirm the presence of any glassy phases that might form. Test samples were sectioned and scanned as illustrated in Figure 4.
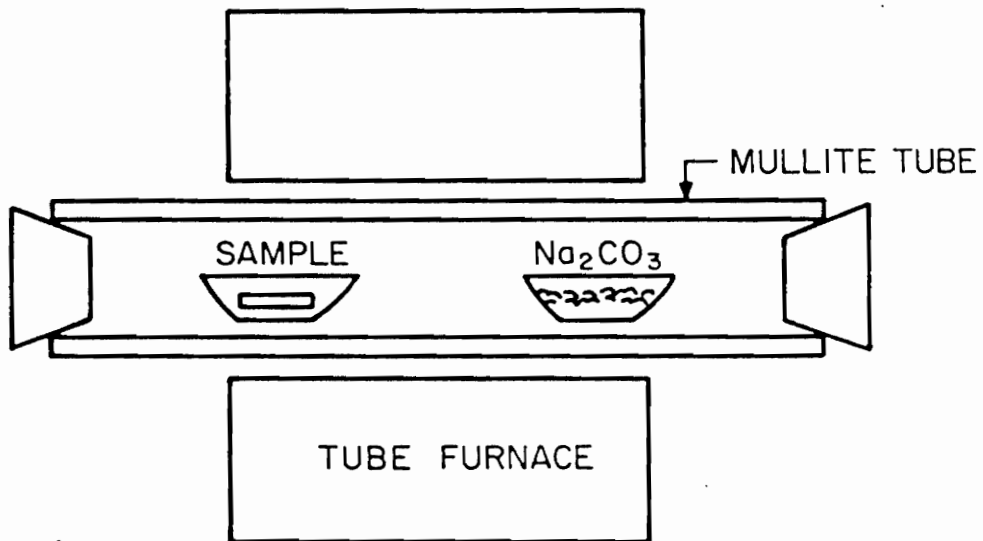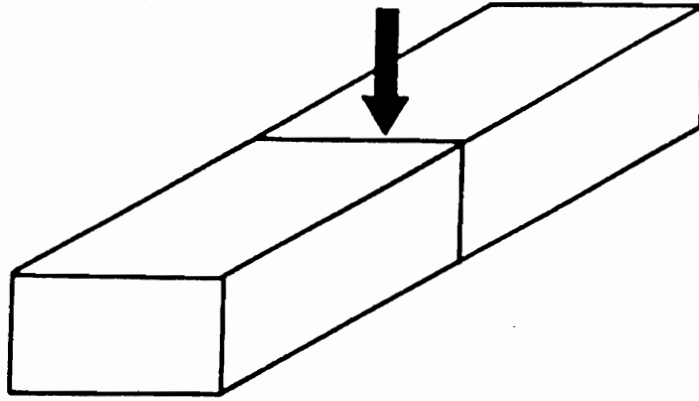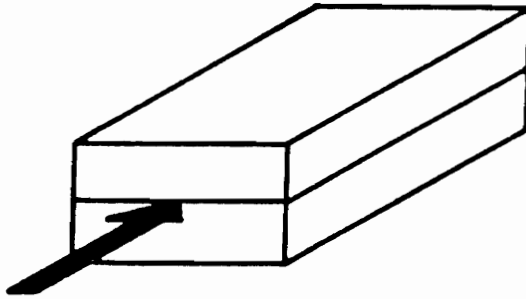
Figure 3. Schematic diagram of alkali exposure test apparatus.

(a) Vertical cutting of exposed test bar.

(b) Horizontal sectioning of cut specimen.

(c) Scanning direction.

Figure 4. Preparation of alkali test specimen for
EDX/SEM examinations.

III. <u>RESULTS AND DISCUSSION</u>

A. Computer Calculations

The results of the computer calculations for the solid phases formed from the reactions ·of sodium impurities with the kaolinite are shown in Table 4. The phases are shown in order of decreasing mole percent. The results illustrate that both temperature and sodium concentration are major factors in determining the extent corrosion of calcined kaolinite except at low temperatures and that sodium compounds readily react with calcined kaolinite except at low temperatures and/or low ratios of Na_2O to Al_2O_3. Results of similar computations carried out with an oxidizing atmosphere indicate that gas phase mixture has little effect on the solid phase equilibria.

The results of the computer calculations for the solid phases formed from the reactions of potassium impurities with the kaolinite are shown in Table 5. The phases are shown in order of decreasing mole percent. The result of these calculation indicate that potassium is not as reactive as sodium at temperature below 925°C. However, at high concentrations and high temperature the potassium exposure would result in complete consumption of both the mullite and the silica.

Table 4. Stable Phases Predicted by
Thermodynamic Calculations for Reactions with Sodium[*]

Temperature	Phases
Ratio of $Al_2O_3:Na_2O = 2:1$	
725°C	$SiO_2, A_3S_2, AS_2, NAS_6$
925°C	$N_2AS_2, NAS_6, SiO_2, A_3S_2$
1225°C	$N_2AS_2, SiO_2, A_3S_2, NS_2$
Ratio of $Al_2O_3:Na_2O = 1:1$	
725°C	$N_2AS_2, SiO_2, A_3S_2, NS, NS_2$
925°C	$N_2AS_2, NS, NAS_6, SiO_2, A_3S_2$
1225°C	$N_2AS_2, SiO_2, A_3S_2, NS_2$
Ratio of $Al_2O_3:Na_2O = 1:2$	
725°C	$N_2AS_2, SiO_2, A_3S_2, NS_2$
925°C	$N_2AS_2, SiO_2, A_3S_2, NS_2$
1225°C	$N_2AS_2, NS_2, SiO_2, A_3S_2$

[*]Conventional Cement Chemistry notation used throughout
tables: $N=Na_2O$ $S=SiO_2$ $A=Al_2O_3$ $K=K_2O$

Table 5. Stable Phases Predicted by
Thermodynamic Calculations for Reactions with Potassium

Temperature	Phases
Ratio of $Al_2O_3:K_2O$ = 2:1	
925°C	SiO_2, A_3S_2, KAS_2
1025°C	$SiO_2, A_3S_2, KAS_2, KAS_6, KS_2$
1225°C	$SiO_2, A_3S_2, KAS_4, KAS_6, KS_2$
Ratio of $Al_2O_3:K_2O$ = 1:1	
925°C	$KAS_4, KAS_2, KAS, SiO_2, A_3S_2$
1025°C	$KAS_2, SiO_2, KS_2, A_3S_2, KA_{S6}$
1225°C	$KAS_4, KS_2, KAS, A_3S_2, KAS_6$
Ratio of $Al_2O_3:K_2O$ = 1:2	
925°C	$KS_2, KAS_2, KAS, KA, KAS_4, SiO_2, A_3S_2$
1025°C	$KS_2, KAS_2, KA, KAS, KAS_4$
1225°C	$KS_2, KAS_2, KA, KAS, KAS_4$

B. Alkali Exposures

1. Kaolinite Exposures to Sodium Vapors

Visual inspection of kaolinite sample bars after exposure to sodium vapor environment revealed little or no damage to the bars at temperatures between 525°C and 800°C.   A glassy coating was observed to have formed on samples exposed to the sodium environment at or above 820°C.

As shown in Table 6, XRD phase analyses of surface and interior portions of surface and interior portions of the kaolinite specimens revealed that only those samples exposed to the sodium containing environment at temperatures of 925°C and 1225°C changed appreciably in mineralogy.   Phase identification results of the reacted zones of these samples indicated the formation of sodium metasilicate and a solid solution of sodium metasilicate and a solid solution of sodium aluminum silicates and carnegieite.

Table 6. Experimentally Determined Kaolinite-Sodium Phases

Reaction Temperature	Stable Phases Surface	Stable Phases Interior
525°C	A_3S_2, SiO_2	A_3S_2, SiO_2
725°C	A_3S_2, SiO_2	A_3S_2, SiO_2
925°C	$NS, NAS, N_2AS_2(ss)$	A_3A_2, SiO_2
1225°C	$NS, NAS, N_2AS_2(ss)$	A_3S_2, SiO_2

A comparison of the experimentally determined phases and the calculated phases, listed in Table 7, shows good agreement. The only conflict observed was the absence of albite (NAS_6) in the experimentally determined phases, possible due to thermodynamic non-equilibrium caused by kinetic hindrances.

In general, the results of both the calculated and experimental determined phases can be predicted by examination of the phase diagram of the SiO_2-Al_2O_3-Na_2O system and the appropriate isoplethel section as shown in Figure 5.

The samples exposed to sodium vapor at the higher temperatures were sectioned and examined using EDX to determine the influence of temperature and time on the depth of alkali diffusion into the kaolinite specimens. Sodium concentration profiles of samples exposed at 925°C and 1225°C are shown in Figures 6 and 7, respectively. At these temperatures, the penetration of sodium was restricted to less than 1 mm due to the rapid formation of a viscous melt and glassy phase. The glassy phase contained 20wt% of Na_2O.

Evidence of the glassy phase was observed when thin sections of samples fired at 925°C and 1225°C for 24 and 12 hours, respectively, were examined optically using a polarizing microscope. The glass phase was found to melt

Table 7. Kaolinite-Sodium Phases

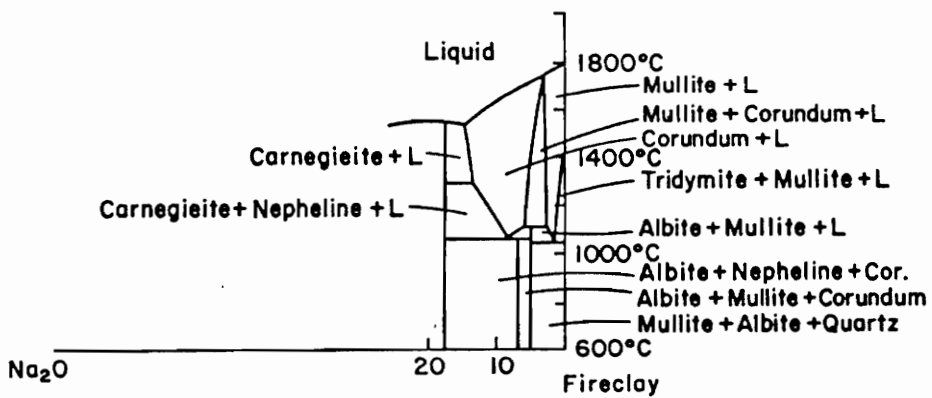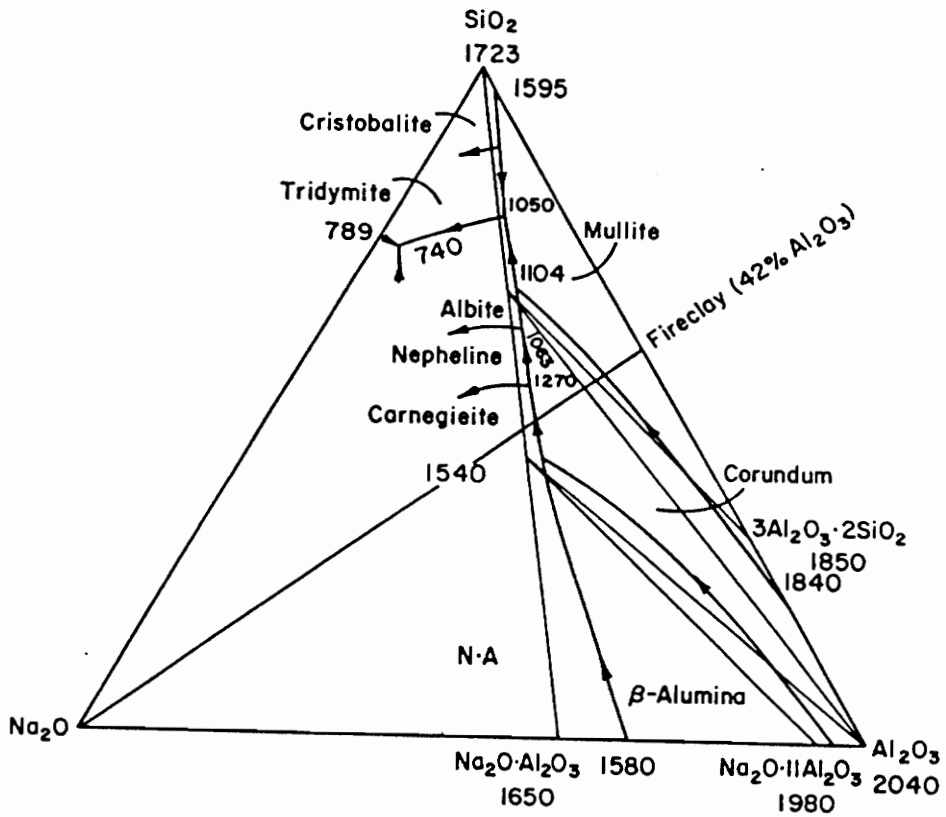| Temperature	Calculated Phases	Experimental Phases
725°C	$SiO_2, A_3S_2, N_2AS_2, N_2AS_6$	SiO_2, A_3S_2
925°C	$N_2AS_2, NS, N_2AS_6, SiO_2, A_3S_2$	$NS, NAS, N_2AS_2(ss), SiO_2, A_3S_2$
1225°C	$N_2AS_2, SiO_2, A_3S_2, NS_2$	$NS, NAS, N_2AS_2(ss), SiO_2, A_3S_2$

Figure 5. Al_2O_3-SiO_2-Na_2O phase diagram and Na_2-fireclay isoplethal section.
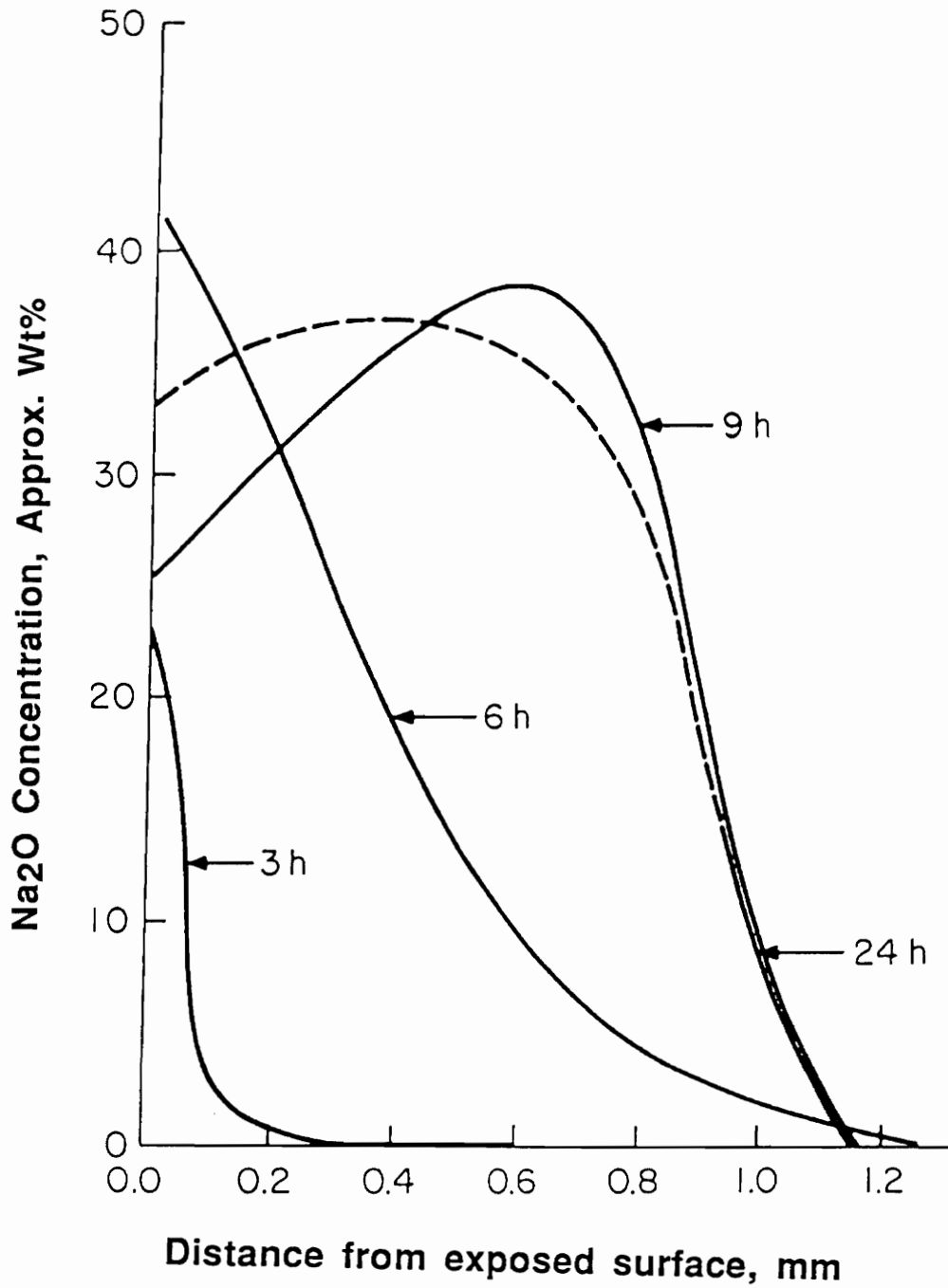
Figure 6. Distribution of sodium oxide in kaolinite sample at 925° C. Note: Concentration data approximated from EDX-SEM results.
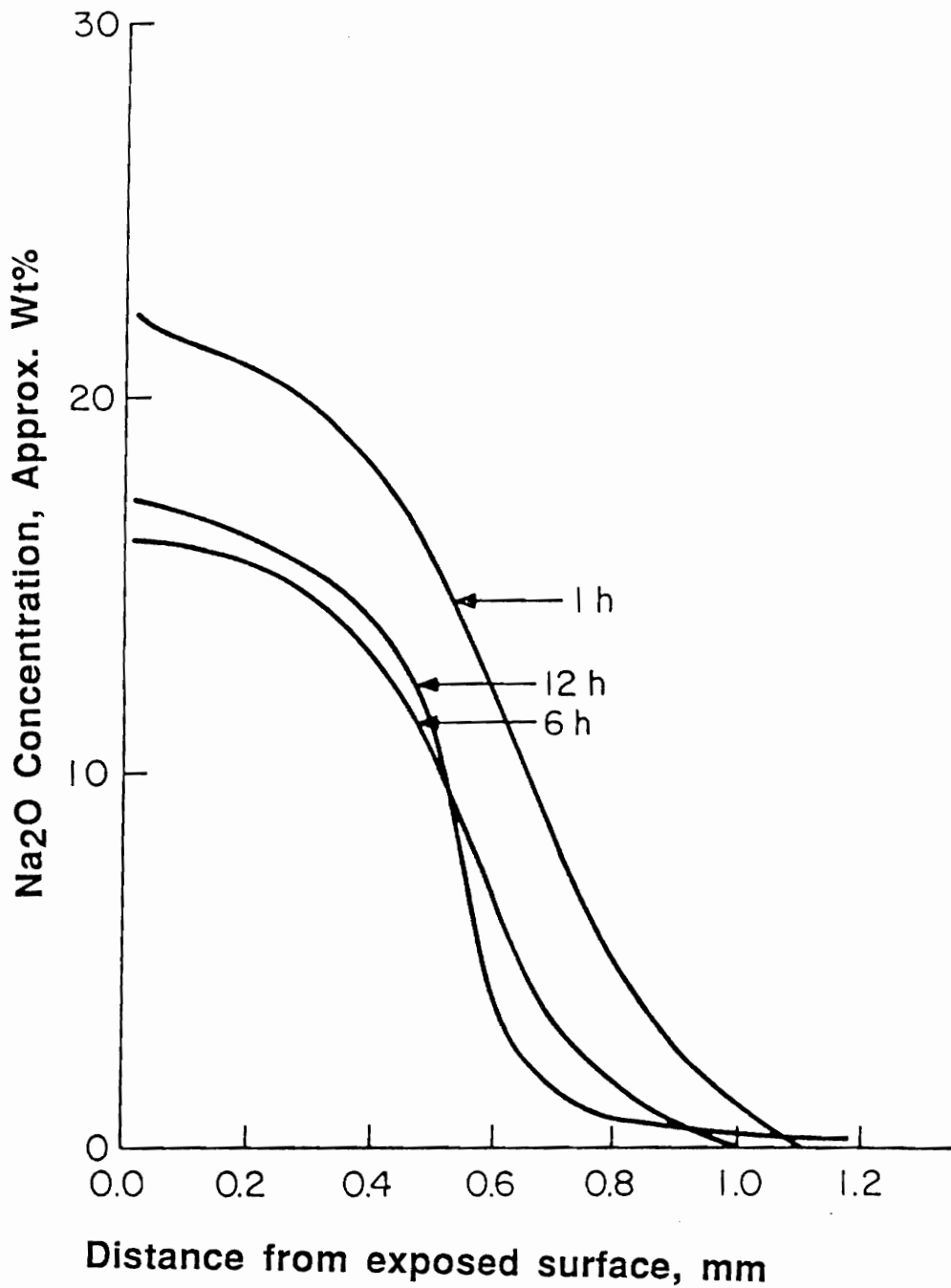
Figure 7. Distribution of sodium oxide in kaolinite sample at 1225° C. Note: Concentration data approximated from EDX-SEM results.

below 1200°C. In the samples fired at 925°C, only a small amount of glass was found. However, the samples fired at 925°C showed a greater depth of sodium penetration (~ 1.2 mm) than those fired at the higher temperature (~ 1.0 mm). The lower firing temperature reduces the rate of reaction of the sodium with the kaolinite and does not allow for the formation of a viscous melt until extremely high concentrations of sodium, approximately 40 wt% of Na_2O, are present.

Further examination of the concentration profiles of samples fired at 925°C indicated the possible depletion of the alkali source for test samples fired for longer than 6 h. This was verified by a weight loss measurement test using 3 g of sodium carbonate. It was found that the sodium source was expended after approximately 30 min at 1225°C and after 7.5 h at 925°C.

A comparison of the sodium distribution profiles for the samples fired at 925°C for different time periods indicates possible spalling and material loss in the sample fired for 24 h. The depth of sodium penetration in this sample was significantly less than that in the other sampled fired at this temperature. The sample fired for 24 h also had a lower maximum concentration of sodium, only 10 wt% Na_2O compared to 40 wt% Na_2O for the other samples exposed at this temperature.

SEM examination of the sample exposed to sodium for 9 h at 925°C verified existence of spalling at the exposed

Exposed
surface

Reaction
boundary

Bulk of
sample

1mm20.1kV 2.64E1 4027/00 PHILIPS
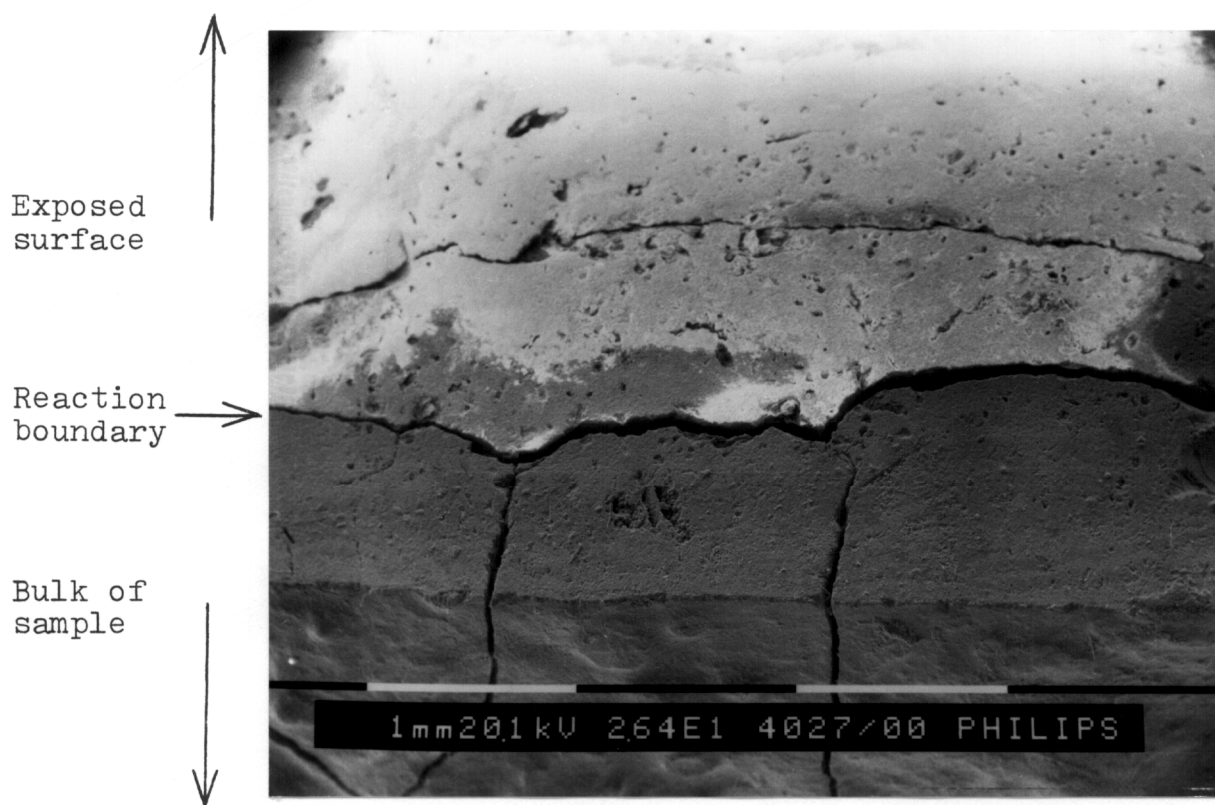
Figure 8.   SEM of fireclay sample exposed to
            sodium vapor showing reaction boundary
            and associated thermal spalling.

surfaces of the specimens. The scanning electron micrograph in Figure 8 reveals cracking parallel to the hot face and eminent spalling in the sample. Therefore, the sodium diffusion profile of the sample fired at 925°C for 24 h (Figure 6) was adjusted to take into account the spalling that occurred; therefore, a portion of the profile was estimated.

The two major variables affecting the diffusion of sodium into kaolinite appear to be time and heat treatment. Length of firing time greatly affects samples fired at 925°C by allowing deeper penetration and possible spalling. This happens because melting does not occur at this temperature until the sodium concentration is very high. At 1225°C, a melt forms which serves as a barrier to the alkali diffusion.

Although the role of temperature in these experiments is not obvious, the rate of diffusion appears to increase with increasing temperature. This is evidenced not only by comparing the 1 h fired at 1225°C to the 3 h firing at 925°C, but also by the increased rate of chemical reaction observed at 1225°C. The increased rate of reaction causes the rapid formation of a viscous melt at 1225°C and therefore seals the surface to further diffusion.

In summary, the results of these experiments indicate that a kaolinite binder material is sensitive to exposure to sodium vapor in combustion atmospheres, even at relatively low temperatures. The alkali phases formed by sodium-kaolinite, e.g., nepheline (low temperature form of carnegieite) has $\alpha = 14.0 \times 10^{-6}/°C$ and calcined kaolinite has $\alpha = 5.1 \times 10^{-6}/°C$. High thermal expansion leads to low thermal shock resistance, causing spalling or cracking with temperature changes. Alternatively, the formation of a ternary glass phase on the surface of the kaolinite samples poses a significant problem due to its low strength and poor thermal shock resistance. Also, the formation of low melting eutectics results in viscous flow of the material and strength determination, and subsequent premature failure.

2. Kaolinite Exposures to Potassium

Visual inspection of the samples bars after exposure to the potassium vapor environment revealed little or no damage at temperatures between 525° C and 900° C. Samples exposed to the alkali environment between 900° C and 1000°C showed some discoloration and slight glazing of the outer surface. The sample exposed to potassium vapors at 1225° C showed significant glazing and discoloration.

As shown in Table 8, XRD phase identification of surface and interior portions of the kaolinite specimens revealed that only those samples exposed to the potassium-containing environment at 1225° C changed

Table 8. Experimentally Determined Kaolinite-Potassium
Phases

Reaction Temperature	Stable Phases, Surface (<1 mm)	Stable Phases, Interior (>1 mm)
925° C	A_3S_2, SiO_2	A_3S_2, SiO_2
950° C	A_3S_2, SiO_2	A_3S_2, SiO_2
1025° C	A_3S_2, SiO_2, KAS_2	A_3S_2, SiO_2
1225° C	KAS_2, KS_2, $K_5A_5S_8$, KA	A_3S_2, SiO_2

appreciably in mineralogy. Only traces of
kaliophilite-nepheline were found at 1000° C, and no
detectable change in mineralogy occurred at lower
temperatures. Phase identification results of the reacted
zones of the sample fired at 1225° C indicated the
formation of potassium disilicate,
kaliophilite-nepheline, potassium aluminate, and
$5K_2O \cdot 5Al_3O_3 \cdot 8SiO_2$.

Good agreement was found between the experimentally
determined phases and the calculated phases, as shown in
Table 9. The lack of either potash feldspar or leucite
formation in the exposed samples is probably due to:
(1) non-equilibrium because the transport of potassium
in the solid phase is inhibited by its relatively large
ionic size compared to that of sodium, and (2) the
relatively low temperature slows the kinetics of the
chemical reactions. The slow transport of potassium will
be further discussed in the next section.

In general, the results of both the calculated and
experimental determined phases can be predicted by
examination of the phase diagram of the SiO_2-Al_2O_3-K_2O
system and the appropriate isoplethel section as shown in
Figure 9.

Table 9. Kaolinite-Potassium Phases

Temperature	Calculated Phases	Experimental Phases
925° C	SiO_2, A_3S_2	SiO_2, A_3S_2
1025° C	SiO_2, A_3S_2, KAS_2, KAS_6, KS_2	SiO_4, A_3S_2, KAS_2
1225° C	KS_2, KAS_2, KA, KAS KAS_4	KS_2, KAS_2, KA, $K_5A_5S_8$

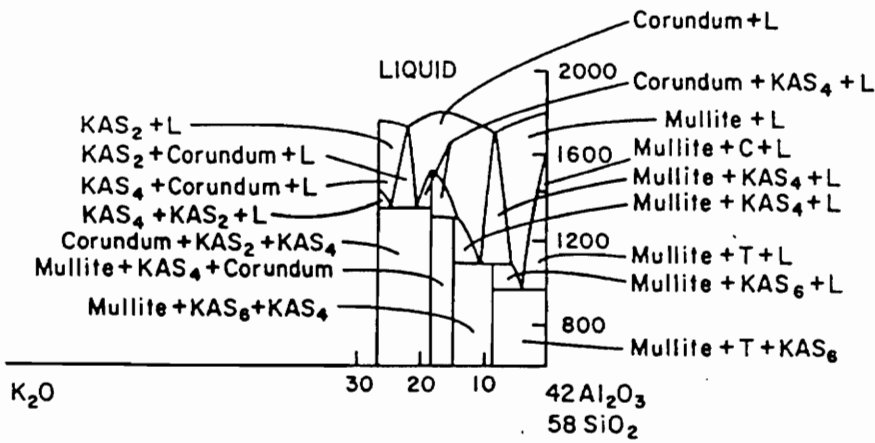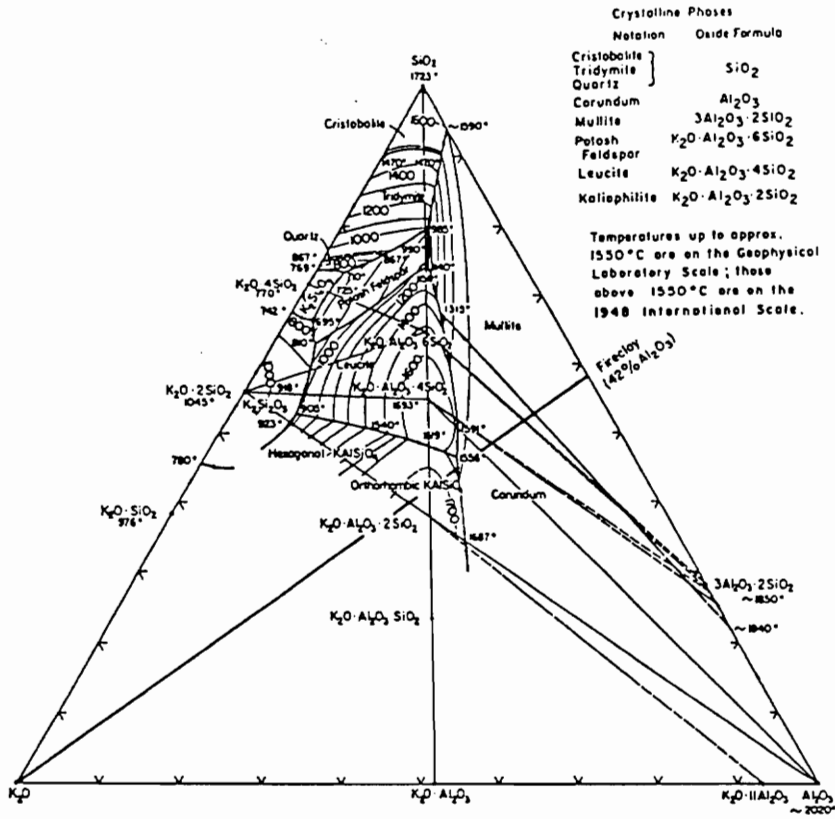Figure 9. Al$_2$O$_3$-SiO$_2$-K$_2$O phase diagram and K$_2$O-fireclay isoplethal section.[33]

Sections of kaolinite samples exposed to potassium vapor were analyzed using EDX to determine the influence of temperature and time on the depth of alkali diffusion. The resulting concentration profiles of samples exposed at 1025° C and 1225° C are shown in Figures 10 and 11, respectively. Potassium penetration into the kaolinite samples was restricted to less than 0.5 mm at 1025° C and to 0.9 mm at 1225° C. Potassium penetration was observed to be significantly less than sodium penetration at 925°C, but roughly comparable at 1225° C. In addition, the depth of penetration of potassium increases with increasing temperature, differing from sodium diffusion where the rapid formation of a melt at 1225° C prevents deep penetration. The formation of a melt did not appear to occur in any samples exposed to potassium vapors, except for the sample exposed at 1225° for 12 h. Potassium oxide concentrations of approximately 40 wt% were detected on the surface of samples exposed for 12 h at both 1025° C and 1225° C.

The diffusion of potassium vapors into the kaolinite specimens appears to be significantly slower than that of sodium under similar conditions. For example, sodium penetrated 1.3 mm into kaolinite in 9 h at 925° C, whereas potassium penetrated only 0.4 mm in 12 h at 1025° and 0.6 mm in 12 h at 1225° C. The diffusion of potassium is believed to be restricted by the relatively large size of
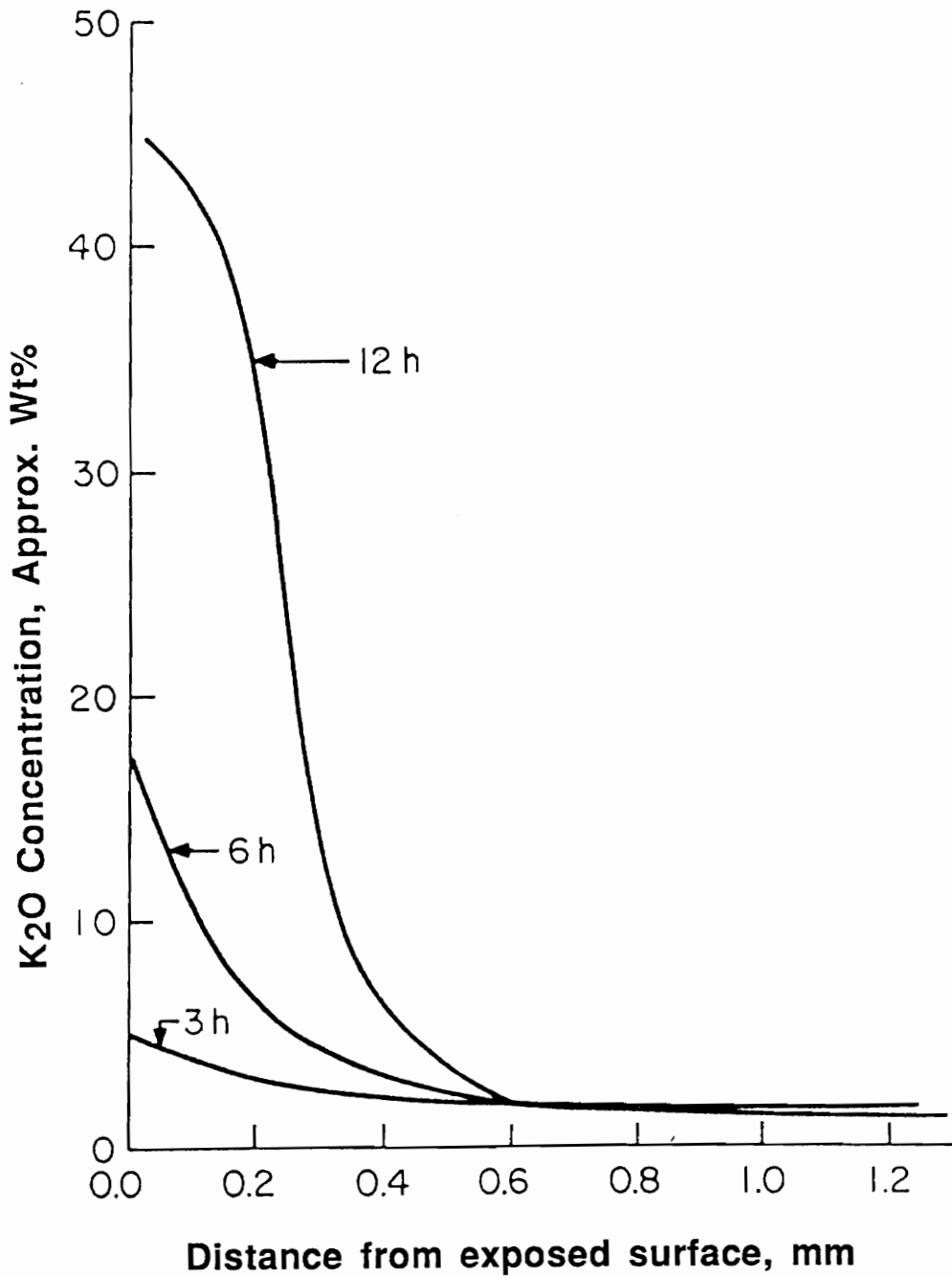
Figure 10.   Distribution of potassium oxide in kaolinite
              sample at 1025° C.   Note: Concentration data
              approximated from EDX-SEM results.
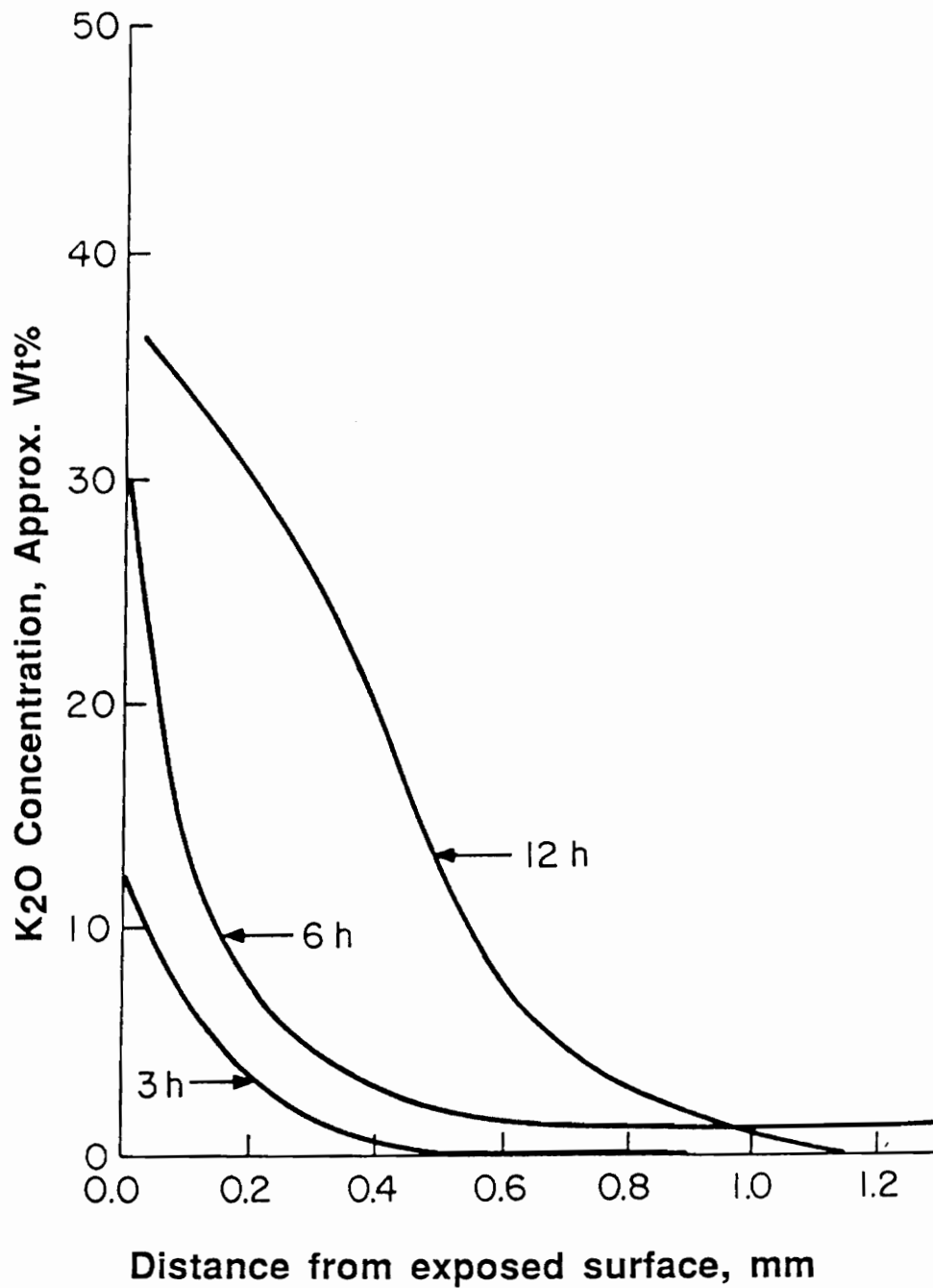
Figure 11.   Distribution of potassium oxide in kaolinite
            sample   at   1225° C.   Note: Concentration data
            approximated from EDX-SEM results.

the potassium cation as compared to the sodium cation.

In summary, the 42% Al_2O_3 calcined kaolinite appears to be a suitable binder material in the presence of potassium vapors at temperatures below 1000° C and possible up to 1225° C for limited periods of time. This appears to be due to the decreased chemical reactivity of the binder material with potassium when compared to sodium, as well as to the inability of potassium to penetrate deeply into the solid phase sample.

3. Mullite Exposures to Potassium and Sodium

Visual inspection of the mullite samples following 6 h exposures to potassium vapors at 1225° C revealed extensive cracking and the specimens disintegrated when sectioning was attempted. The sample exposed to potassium vapors for 6 h at 1025° C was completely destroyed, as shown in Figure 12. XRD analyses of the test samples showed that significant amounts of potassium aluminate had formed along with kaliophilite-nepheline. The large volume expansion associated with the formations of these compounds is believed to be the main cause of the complete destruction of the sample bars.

The mullite sample bars were also exposed to sodium vapors at 925° C for 6 h. Visual examination of the exposed bars showed little damage, but an apparent volume expansion has occurred. XRD analyses of these bars revealed that significant changes in the mineralogy had occurred. Phases identified were primarily carnegieite
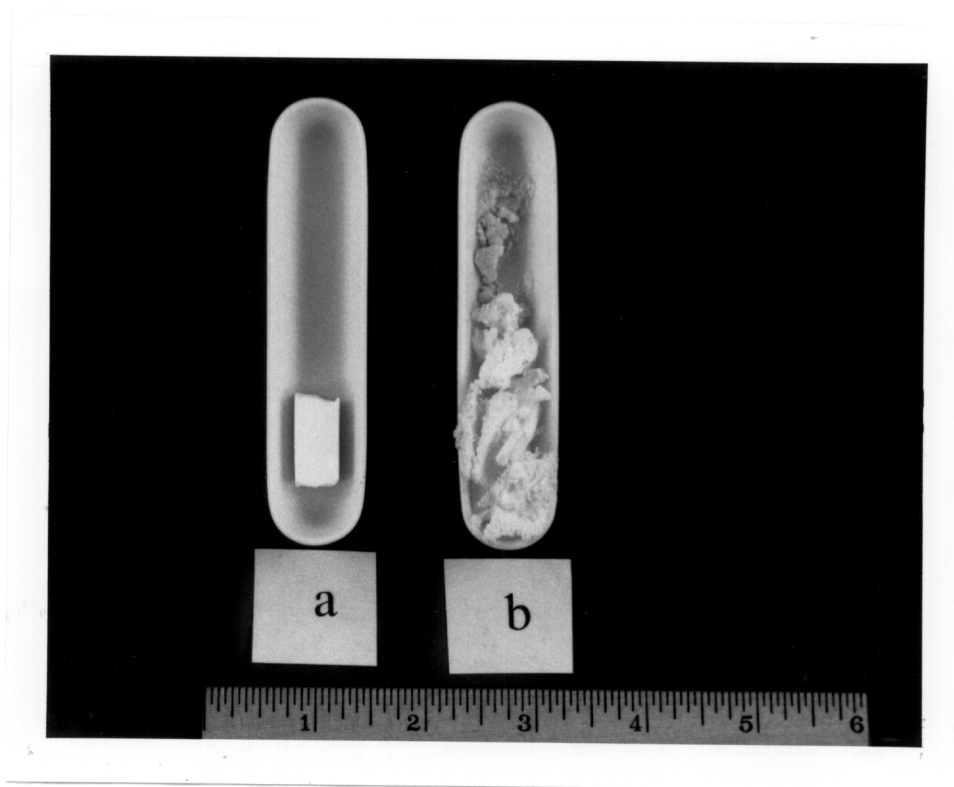
Figure 12. Mullite (60% Al_2O_3) samples (a) before exposure, and (b) following 6 h exposure to potassium at 1025 C.

and a sodium aluminosilicate solid solution with only trace amounts of mullite present.

The results of these experiments indicate that the 60% Al_2O_3 aluminosilicate material is prone to failure in alkali-containing environments at temperatures of 925° C to 1225° C.

IV. CONCLUSIONS

The results of these experiments can be summarized as follows:

1) Sodium compounds penetrate rapidly in 42% alumina alumiosilicates at temperatures between 925°C and 1225°C. Significant changes in minerology occur in the region penetrated by sodium. The formation of low melting eutecitics and expansive phases occur rapidly in areas penetrated by sodium.

2) Potassium compounds are not a significant source of alkali attack for the 42% alumina aluminosilicate at temperatures below 1025°C. Only limited minerology changes occurred in areas penetrated by potassium at 1025°C. Penetration of potassium was also limited at 1025°C to less then 0.5 mm even after 12h of exposure.

3) The computer program SOLGASMIX-PV in conjunction with phase diagrams can be used successfully to predict the solid phase equilibria in ceramic systems.

4) The use of a 42% alumina aluminosilicate as a binder material is recommended for operating temperatures below 800°C.

V. RECOMMENDATIONS FOR FURTHER RESEARCH

1) Exposure of ceramic filter material to an alkali-contaning environment with the purpose of correlating strength loss with exposure time.

2) A study of the kinetics of sodium and potassium reactions with aluminosilicates. This information would be useful in determining failure times for those materials that do not form a surface melt.

REFERENCES

1. C.R. Kennedy, "Alkali Attack on a Mullite Refractory in the Grand Forks Energy Technology Center Slagging Gasifier," <u>Journal of Materials for Energy Systems</u>, Vol. 3, June, 1981, p.27

2. D.R.Diercks and D.Stahl, "A Review of Refractory Materials for the Memphis Industrial Fuel Gas Demonstration Plant," ANL/FE-81-60,Argonne, Illinois, Argonne National Laboratory, September, 1981.

3. G.C. Wei, V.J. Tennery, and L.A. Harris, "Effects of Alternate Fuels Report No. 1, Analysis of High-Duty Fireclay Refractories Exposed to Coal Combustion," ORNL/TM-5909, December, 1977.

4. R.F. Hayden, "Study of the Resistance of Refractories to Alkali Vapors," Master's Thesis, Virginia Polytechnic Institute and State University, May 1976.

5. R.E. Farris, and J.E. Allen, "Aluminous Refractories Alkali Reactions," <u>Iron and Steel Engineer</u>,February, 1973, pp. 67-74.

6. P.H. Havranek, "Alkali Attck on Blast Furnace Refractories," <u>Journal of British Ceramic Society Transactions</u>, V. 77, (3), pp. 92-97, 1978.

7. G.R. Rigby, and R. Hutton, "Actions of Alkali and Alkali-Vanadium Oxide Slags on Alumina-Silica Refractories, "<u>J.Am. Ceram. Soc.</u>, Vol. 45, No. 12, 1962, pp. 68-73.

8. J.I. Federer and V.J. Tennery, "Effects of Aternate Fuels, Report No. 7: Analysis of Failure of a Mullite-Based Refractory Brick in an Industrial Oil-Fired Burner," ORNL/TM-6878, July, 1979.

9. J.I. Federer, "Corrosion of Materials by High Temperature Industrial Combustion Environments - A Summary," ORNL/TM--9903, February, 1986.

10. T.M. Besmann, "SOLGASMIX-PV, A Computer Program to Calculate Equilibrium Relationships in Complex Chemical Systems," ORNL/TM-5775, Contract No. W-7405-eng-26, April, 1977.

11. T. Sun, "Alkali Attack of Coal Gasifier Refractory Linings," Master Thesis, Virginia Polytechnic Institute and State University, June, 1986.

12. K. Lee, "Alkali Attack on Coal Gasifier Refractory Lining," Master Thesis, Virginia Polytechnic Institute and State University, May, 1988.

13. T.C. Tiearney, Jr., and K. Natesan, "Metallic Corrosion in Simulated Low-Btu Coal-Gasificatoin Atmosphere," J. Materials for Energy Systems, Vol. 1, March 1980, p. 13.

14. A.R. Fichar, S.H. Bruce, and R.F. James, "Thermodynamic Properties of Minerals and Related Substances at 298.15K and 1 Bar Pressure and at High Temperatures," U.S. Geol. Survey Bull. 1452, 1979.

15. E.T. Turkdogan, "Selected Thermodynamic Functions, "Physical Chemistry of High Temperature Technology, Academic Press, 1980.

16. JANAF Joint Army, Navy, Air Force Thermochemical Tables, 2nd ed., 1971, NSRDS-NBS 37, US Government Printing Office: Washington, DC.

17. JANAF Thermochemical Tables, Nat. Bur. Stand., Washington, 1978.

18. M.W. Chase, Jr., J.L. Curnutt, A.T. Hu, H. Prophet, A.N. Syverud, and L.C. Walker, "JANAF Thermochemic Tables," 1974 Supplement, J. Phys, Chem, Ref. Data, Vol. 3, No. 2, p.311, 1974.

19. M.W. Chase, Jr., J.L. Curnutt, H. Prophet, R.A. McDonald, and A.N. Syverud, "JANAF Thermochemic Tables," 1974 Supplement, J. Phys, Chem, Ref. Data, Vol. 4, No. 1, p. 1, 1975.
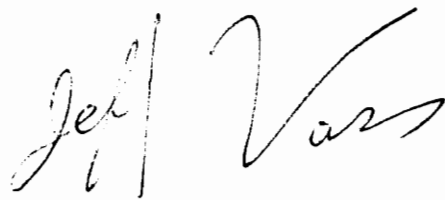
20. M.W. Chase, Jr., J.L. Curnutt, R.A. McDonald, and A.N. Syverud, "JANAF Thermochemic Tables," 1978 Supplement, _J. Phys, Chem, Ref. Data_, Vol. 7, No. 3, p. 793, 1978.

21. M.W. Chase, Jr., J.L. Curnutt,. J.R. Downey, R.A. McDonald, A.N. Syverud, and E.A. Valenzuela, "JANAF Thermochemic Tables," 1982 Supplement, _J. Phys, Chem, Ref. Data_, Vol. 11, No. 3, p. 695, 1982.

22. M.W. Chase, Jr., C.A. Davies, J.R. Downey, Jr., D.J. Frurip, R.A. McDonald, and A.N. Syverud, _JANAF Thermochemical Tables, Third Edition,_ Am. Chem Soc. and Am. Ins. Phys, for Nat. Bur. Stand., Vol. 14, 1985.

23. I. Barin, O. Knacke, and O. Kubaschewski, _Thermochemical Properties of Inorganic Substances,_ Supplement, Springer-Veriag, Berlin and New York, 1977.

24. O. Kubaschewski, E.L. Evans, and C.B. Alcok, "Metallurgical Thermochemistry," Pergamon, Oxford, 1967.

25. I. Barin, O. Knacke, and O. Kubaschewski, _Thermochemical Properties of Inorganic Substances,_ Supplement, Springer-Veriag, Berlin and New York, 1973.

26. K.K. Kelley, S.S. Todd, F.L. Orr, E.G. King, and K.R. Bonnickson, "Thermodynamic Properties of Sodium-Aluminum and Potassium-Aluminum Silicates," _U.S. Bur. Mines, Report of Investigations 4955._

27. R.P. Beyer, M.J. Ferrante, R.R. Brown, and G.E. Daut, "Thermodynamic Properties of Potassium Metasilicate and Disilicate," _U.S. Bur. Mines. Report of Investigations 5901._

28. R.P. Beyer, M.J. Ferrante, R.R. Brown, and G.E. Daut, "Thermodynamic Properties of $KAlO_2$," _J. Chem Thermodynamics_, Vol. 12, 1980, p. 985.

29. J.W. Hastie, W.S. Horton, E.R. Plante, and D.W. Bonnell, "Thermodynamic Models of Alkali-Metal Vapor Transport in Silicate System," High Temp.-High Pressures, Vol. 14, 1982, p. 669.

30. B.I. Arlynk, "Determination of the Heats of Formation of a Number of Compounds by Quantitiative Thermal Analysis," English translation of Zhur. Priklad. Khim., Vol. 41, No. 4, April 1968, p. 783.

31. J.T. Kummer, "β-Alumina Electrolytes," Progr. Solid State Chem., Vol. 7, 1972, p.141.

32. Y.Y. Skolis, V.A. Levitskii, and V.M. Yanishevskii, "Thermodynamics of Binary Oxides. Thermodynamic Properties of $CaAl_4O_7$ and $CaAl_{12}O_{19}$ at High Temperatures," Russian Journal of Physical Chemistry, Vol. 55, 1981, p. 25.

33. E.M. Levin, C.R. Robbins, and H.R. McMurdie, Phase Diagrams for Ceramists, p. 156, American Ceramic Society, Inc.,Colombus, Ohio (1964).

VITA

Raymond Jeffrey Vass was born in Philadelphia, Pennsylvania on August 26, 1960. He attended Bullis School in Potomac, Maryland and Blair Academy in Blairstown, New Jersey. He received a Bachelor of Chemical Engineering from the University of Delaware in June of 1984.

The author began graduate work at Virginia Polytechnic Institute and State University in August 1987 and completed the requirements for the Master of Science degree in Fall 1990. His work experience includes working at the Federal Energy Regulatory Commission as an engineer.

47